Keysight Technologies
Several Aspects of High Resolution Imaging in Atomic Force Microscopy

Application Note

High-resolution imaging has been the primary feature that attracted the researchers' attention to scanning probe microscopy yet there are still a number of outstanding questions regarding this function of scanning tunneling microscopes and atomic force microscopes. Here I would like to address a few related issues starting with AFM imaging of alkane layers on graphite. Normal alkanes (chemical formula C_nH_{2n+2}) are linear molecules with a preferential zigzag conformation of the -CH_2- groups. The terminal -CH_3 groups are slightly larger than -CH_2- groups but more mobile. At ambient conditions the alkanes with *n=18* and higher are solid crystals (melting temperature of $C_{18}H_{38}$ – 28°C) with the chains oriented practically vertical to the larger faces of the crystals. Such surface of the $C_{36}H_{74}$ crystal, which is formed of -CH_3 groups, was examined in contact mode, and the AFM images revealed the periodical arrangement of these groups [1]. It has been known for a long time that on the surface of graphite the alkane molecules are assembled in flat-laying lamellar structures, in which the fully extended molecules are oriented along three main graphite directions, Fig. 1. This molecular order is characterized by a number of periodicities: the 0.13nm spacing between the neighboring carbon atoms, the 0.25nm spacing between the -CH_2- groups along the chain in the zigzag conformation, the 0.5nm interchain distance inside the lamellae and the lamellae width—the length of the extended C_nH_{2n+2} molecule. The latter varies from 2.3nm for $C_{18}H_{38}$ to 49.5nm for $C_{390}H_{782}$ (the longest alkane synthesized).

The alkane adsorbates on graphite were first examined with STM [2]. In such experiments a droplet of saturated alkane solution is deposited on graphite surface and the metallic tip penetrates this droplet and a molecular adsorbate at the liquid-solid interface until it detects a tunneling current. At these conditions the tip is scanning over the ordered molecular layer in immediate vicinity of the substrate. Such STM images of normal alkanes on graphite (as one reproduced from the paper [3] and presented in Fig. 2) clearly demonstrate the fine details of the molecular arrangement such as the lamellar edges, individual chains inside lamellae and the zigzag conformation of the alkane chains. A specific feature of the STM imaging at the liquid-solid interface is that the probe is surrounded by the alkane saturated solution. Any instability of the imaging and the use of low tunneling gap resistance cause a mechanical damage of the alkane order, and the probe might record the image of the underlying graphite. If the gap is increased again the alkane order

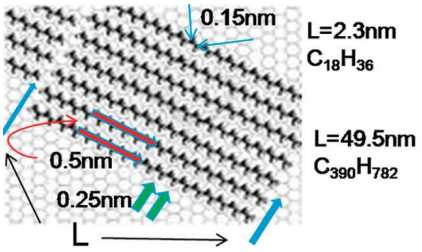

Figure 1. Sketch showing lamellar and molecular order of normal alkane on graphite.

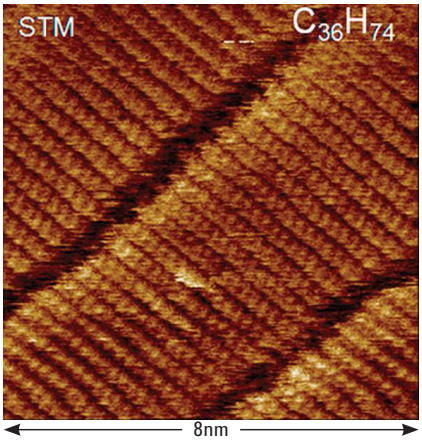

Figure 2. STM image of $C_{36}H_{74}$ alkanes on graphite.

KEYSIGHT TECHNOLOGIES

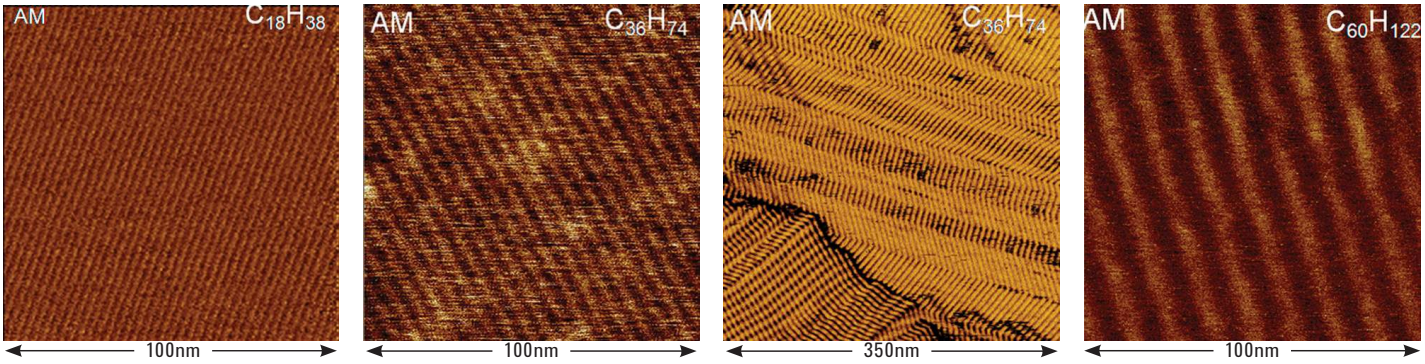

Figure 3. AFM images of normal alkanes on graphite obtained in amplitude modulation mode.

is restored due to a pool of the alkane molecules. It is practically impossible to get STM images of "dry" alkane layers on graphite because an occasional damage of the layer will be non-repairable.

Studies of dry alkane layers on graphite can be performed with AFM but the "STM" resolution of the lamellae arrangement has not been achieved so far. Initially, the lamellar adsorbates of $C_{60}H_{122}$ on graphite were examined in amplitude modulation mode and the spacing of 7.6nm on different lamellar planes and multilayered structures is clearly seen in the images[4]. These periodical structures can be employed for the X- and Y- axis calibration of the scanners in lack of the standards for the few nanometers range. For a while the detection of such images was considered as the demonstration of the high resolution imaging by a particular scanning probe microscope. The visualization of the 7.6-nm strips is not challenging anymore and getting images of smaller lamellar structures of $C_{36}H_{74}$ (4.5nm spacing) and $C_{18}H_{38}$ (2.3nm spacing) can be considered as proof of the microscope performance and the operator experience. Typical AFM images of $C_{18}H_{38}$, $C_{36}H_{74}$ and $C_{60}H_{122}$ lamellae on graphite obtained with the 5500 microscope are shown in Fig. 3. The lamellar edges are clearly resolved in these images. The origin of the contrast is the difference of the effective stiffness of the lamellar core (-CH_2- sequences) and its edges (-CH_3 and nearby -CH_2- groups). A complex pattern of $C_{36}H_{78}$ lamellae seen in the 350-nm image is caused by the grains of the substrate and peculiarities of the chain order inside lamellae. In some sample preparations the neighboring chains are shifted to better accommodate the bulky -CH_3 end groups and this leads to the chains' tilt in respect to the lamellar edges. Therefore the individual lamellae width might be smaller than the length of alkane chains.

Having in mind the STM images of the normal alkanes on graphite, it is rather curious if such resolution can be achieved in AFM: either in the contact or in the oscillatory (amplitude modulation - AM and frequency modulation - FM) modes. There is definite progress in this respect as it is demonstrated with AFM images of three different alkanes ($C_{18}H_{38}$, $C_{242}H_{486}$ and $C_{390}H_{782}$) on graphite obtained in the contact mode, Figs. 4-5. The spacings, which are related to the lamellae and individual chains, are distinguished in the image of $C_{18}H_{38}$ lamellae, Fig. 4 (left). The zigzag pattern along the closely packed alkane chains is seen in the image of the ultra long alkane – $C_{390}H_{782}$, Fig. 4 (right). Several slightly twisted lamellae were detected in the images of $C_{242}H_{486}$, Figs. 5. A number of linear defects

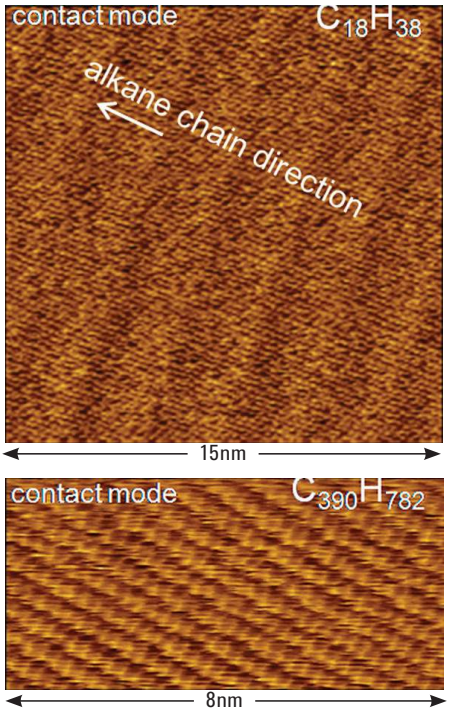

Figure 4. AFM images of $C_{18}H_{38}$ and $C_{390}H_{782}$ lamellae on graphite obtained in the contact mode.

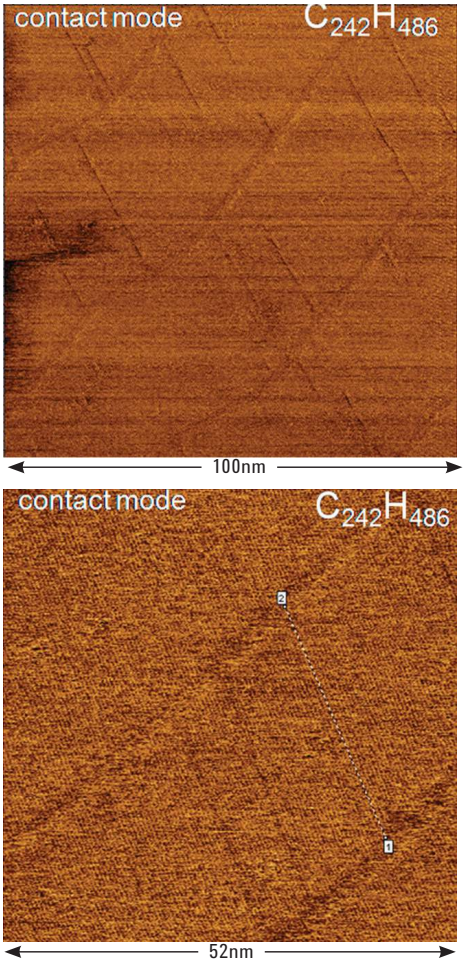

Figure 5. AFM images of $C_{242}H_{486}$ lamellae on graphite obtained in the contact mode.

caused by the missing chains or their parts are also distinguished in the 100-nm image. The individual alkane chains, which are extended between the edges of the lamellae, are also noticed in the 55-nm image.

The collection of high-density images with a number of pixels from 1K to 4K is needed for observations of the lamellar edges and individual chains of long alkanes within the same image. Such imaging takes time and requires the low-thermal drift of the instrument. The demonstrated visualization of the molecular spacing down to 0.25 nm in the contact mode gives us a hope that similar observations can be achieved in the oscillatory AM and FM modes when they are applied in ambient conditions or under the liquid. The 0.25 nm resolution in visualization of the molecular structure of pentacene was been already achieved in the FM experiments in UHV and at low temperatures [5].

For a number of years, the progress in AFM is in part related to the developments and applications of FM mode. Nowadays this technique, which was originally employed in UHV as the alternative (to AM) way of detection tip-sample force interactions and scanning, is also used for high-resolution imaging in air and under liquid. The high-resolution images of mica, self-assemblies of alkanethiols, and polydiacetylene (PDA) crystals were recorded with FM using the home-made set-ups [6–7]. These periodical structures are characterized by spacings above 0.5 nm and in some cases the molecular-scale individual defects were observed. The similar findings were reported with AM mode [8]. Several high-resolution images, which were obtained in AM with the 5500 microscope, are shown at the right.

A number of molecular-resolution images in AM mode were obtained in air on surface of PDA crystal. This crystal can be cleaved and the largest atomically-smooth face of the PDA crystal with few linear defects (Fig. 6, top right) is most suitable for molecular-scale imaging. At higher magnification, the periodical pattern mimicking the crystalline structure of the bc-plane can be obtained, Figs. 6 (top right and bottom). This lattice with the orthogonal spacings of 0.5 nm

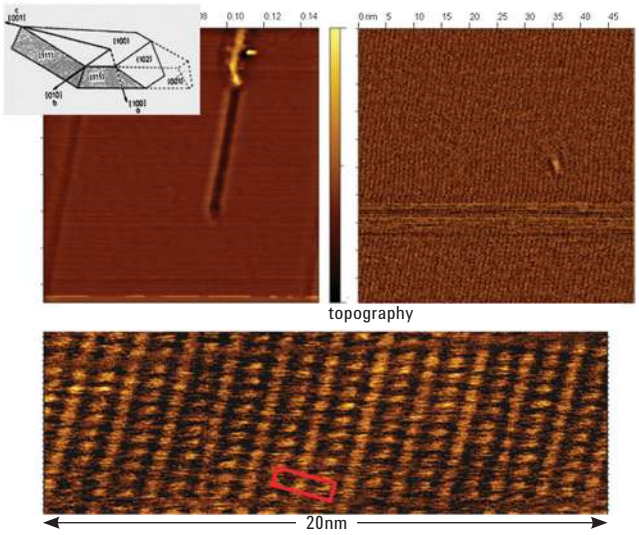

Figure 6. AFM images of polydiacetylene crystal obtained in amplitude modulation mode in air. A red rectangle indicates the crystallographic lattice on the ***bc***-plane of this crystal.

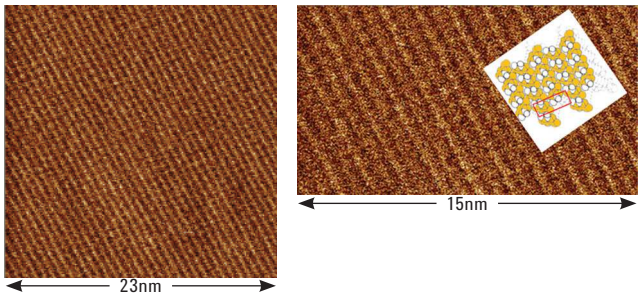

Figure 7. AFM images of polydiacetylene crystal obtained in amplitude modulation mode in air. The probe was different from that in the experiment in Figure 6.

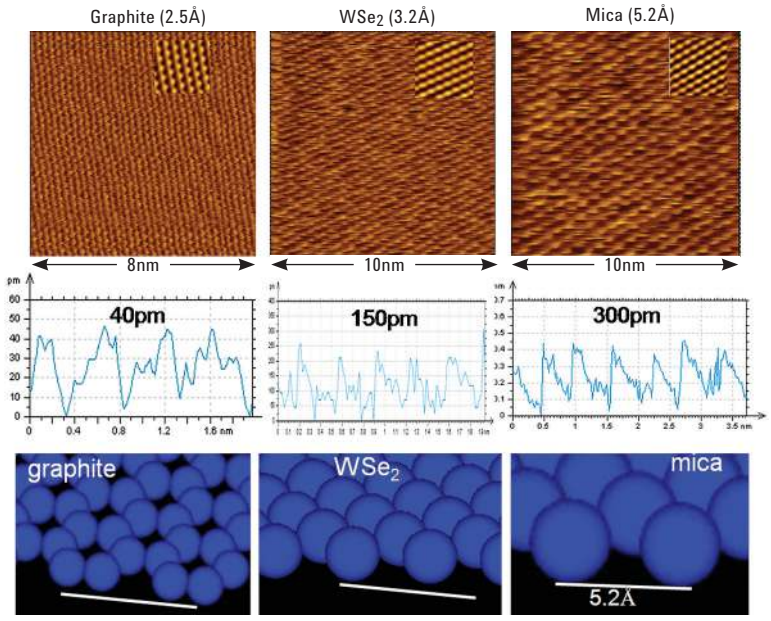

Figure 8. Top row – topography images of three layered crystals obtained in the contact AFM mode. The topography contours along these images are presented underneath them in the middle row. Bottom row – 3D representations of the crystallographic surface structure of carbon, Se and potassium atoms.

(the repeat distance along the c-axis) and 0.7 nm (a half of the repeat distance along the ***b***-axis) is detected in the experiments with different probes, Figs. 7. Despite the similarity of the image patterns obtained with different probes the image variations are noticeable and there is definitely a lack of high-resolution of fine atomic-scale features. The latter is the common feature of the images obtained in AM and FM modes in air and under liquid is that the spacings smaller than 0.5 nm are poorly resolved. The situation is only slightly better for the images in the contact mode, where in addition to visualization of mica surface the lattices of MoS_2 or graphite can be also observed. The contact mode images of these layered materials are shown in Figs. 8. The original images are quite noisy and the periodical lattices can be enhanced with FFT procedure that leads to perfect hexagonal patterns, which are imbedded in the top part of the images. The topography traces along the images are presented underneath, and they show that the surface corrugations increase from 40 pm (graphite) to 300 pm (mica). Therefore, the molecular-scale imaging of mica is less demanding due to the larger corrugations and interatomic separations as seen from the 3D sketches of the atomic surface structure of the crystals (see the bottom of Figs. 8).

In summary, the current status of the atomic-scale imaging in AFM is not satisfactory and there is a room for further improvements. The progress of the high-resolution imaging in the oscillatory AM and FM modes is most desirable because these modes can be applied to much broader range of materials including soft objects as compared with the contact mode AFM. This progress relies on instrumental improvements (better signal-to-noise characteristics, low thermal drift, improved detection and control of the tip-sample forces, etc.) and the use of sharp probes. The other issue is related to the better understanding of the nature of atomic-scale resolution in AFM, which is discussed since first successful visualization of atomic- and molecular-scale lattices in the contact mode. In this mode the single atomic-scale defects have never been practically recorded. Therefore, such imaging provides only the lattice resolution in the contrast to true atomic resolution where a detection of such defects is expected. The imaging of the periodical lattices with the defects was later demonstrated in FM and AM images (first in UHV and later in ambient conditions) yet the results of the computer simulation revealed that visualization of the defects does not necessarily mean that the surrounding molecular order is correctly reproduced in the images [9–10]. These findings emphasize a need of a thorough interplay between the experiment and theory in the analysis of the atomic-scale data.

References

1. W. Stocker et al Polym. Bull. 1991, *26*, 215–222
2. G. C. McGonigal, R. H. Bernhardt, and D. J. Thomson, *Appl. Phys. Lett.* 1990, 57, 28.
3. W. Liang et al *Adv. Mater.* 1993, 5, 817–821.
4. S. N. Magonov, and N. A. Yerina *Langmuir* 2003, 19, 500–504.
5. L. Gross et al, Science 2009, 324, 142.
6. T. Fukuma et. al. *Appl. Phys.* Lett. 2005, 86, 193108.
7. T. Fukuma et. al. *Appl. Phys. Lett.* 2005, 86, 034103.
8. D. Klinov, and S. Magonov *Appl. Phys. Lett*. 2004, 84, 2697.
9. S. Belikov, and S. Magonov *Jap. Jour. Appl. Phys.* 2006, 45, 2158.
10. S. Belikov, and S. Magonov *Proc. Amer. Control Soc.*, St. Louis, 2009, 979.

For more information on Keysight Technologies' products, applications or services, please contact your local Keysight office. The complete list is available at: www.keysight.com/find/contactus

Americas

Canada	(877) 894 4414
Brazil	55 11 3351 7010
Mexico	001 800 254 2440
United States	(800) 829 4444

Asia Pacific

Australia	1 800 629 485
China	800 810 0189
Hong Kong	800 938 693
India	1 800 112 929
Japan	0120 (421) 345
Korea	080 769 0800
Malaysia	1 800 888 848
Singapore	1 800 375 8100
Taiwan	0800 047 866
Other AP Countries	(65) 6375 8100

Europe & Middle East

Austria	0800 001122
Belgium	0800 58580
Finland	0800 523252
France	0805 980333
Germany	0800 6270999
Ireland	1800 832700
Israel	1 809 343051
Italy	800 599100
Luxembourg	+32 800 58580
Netherlands	0800 0233200
Russia	8800 5009286
Spain	0800 000154
Sweden	0200 882255
Switzerland	0800 805353 Opt. 1 (DE) Opt. 2 (FR) Opt. 3 (IT)
United Kingdom	0800 0260637

For other unlisted countries:
www.keysight.com/find/contactus
(BP-07-10-14)

www.keysight.com/find/afm

This information is subject to change without notice.
© Keysight Technologies, 2010 - 2014

Published in USA, July 31, 2014
5990-5479EN
www.keysight.com